

Received: 2016.12.22
Accepted: 2017.01.09
Published: 2017.01.27

Combination of Magnetic Resonance Angiography and Computational Fluid Dynamics May Predict the Risk of Stroke in Patients with Asymptomatic Carotid Plaques

Authors' Contribution:
Study Design A
Data Collection B
Statistical Analysis C
Data Interpretation D
Manuscript Preparation E
Literature Search F
Funds Collection G

ADEF 1,2 Qian Jia
A 1 Hongbin Liu
B 1,3 Yanping Li
C 1 Xiaoxi Wang
B 4 Jinju Jia
BF 5 Yuying Li

1 Second Department of Geriatric Cardiology, Chinese PLA General Hospital, Beijing, P.R. China
2 Department of Cardiology, School of Medicine, Nankai University, Tianjin, P.R. China
3 Outpatient Department of North China Military Materials Procurement Bureau, Tianjin, P.R. China
4 Department of Cardiology, Jizhong Energy Xingtai Mig General Hospital, Xingtai, Hebei, P.R. China
5 Department of Radiology, Chinese PLA General Hospital, Beijing, P.R. China

Corresponding Author: Hongbin Liu, e-mail: hongbinliu301@126.com
Source of support: Departmental sources

Background: Atherosclerosis plaques in the carotid arteries frequently have been found in patients with stroke. However, the pathogenesis of carotid plaque from asymptomatic to cerebrovascular events is a complex process which is still not completely understood. We aimed to investigate the prognosis of asymptomatic carotid atherosclerotic plaques by use of magnetic resonance angiography (MRA) combined with computational fluid dynamics (CFD).

Material/Methods: We prospectively studied a cohort of 228 participants (mean age 59.21±8.48) with asymptomatic carotid atherosclerotic plaques; mean follow-up duration was 1147.56±224.84 days. Plaque morphology parameters were obtained by MRA analysis. Lumen area (LA) and total vessel area (TVA) were measured, and wall area (WA=TVA-LA) and normalized wall area index (NWI=WA/TVA) were calculated. CFD analysis was performed to evaluate hemodynamic characteristics, including wall pressure (WP) and wall shear stress (WSS). Independent risk factors for stroke were obtained by Cox regression analysis. The area under the curve (AUC) of receiver operator characteristic (ROC) and Z-statistic test were used to evaluate risk factors.

Results: Logistics regression analysis showed NWI (OR: 3.472, 95% CI: 2.943-4.096, $P=0.11$) and WSS (OR: 6.974, 95% CI: 1.070-45.453, $P=0.42$) were independent risk factors of stroke for patients with asymptomatic carotid plaques. The area under the ROC curve values for WSS, NWI, and WSS+NWI were 0.772, 0.798, and 0.903, respectively.

Conclusions: The combination of plaque morphology characteristics NWI and hemodynamic parameter WSS may predict the risk of stroke in patients with asymptomatic carotid plaques.

MeSH Keywords: **Atherosclerosis • Carotid Arteries • Magnetic Resonance Angiography • Stroke**

Full-text PDF: <http://www.medscimonit.com/abstract/index/idArt/902995>

 2918  4  6  45



Background

Asymptomatic carotid plaques are very commonly encountered in daily clinical practice, with prevalence ranging from 0.1% to 7.5% in the general population [1]. Atherosclerotic plaques in the carotid arteries are frequently found in stroke patients [2,3]. Asymptomatic carotid stenosis refers to narrowing of the carotid artery caused by atherosclerosis in patients who have not experienced a stroke or transient ischemic attack in the territory of that artery. The pathogenesis of carotid plaque from asymptomatic to cerebrovascular events is a complex process which is still not completely understood. Although many systemic risk factors predispose to development of atherosclerosis, plaque is not uniformly distributed in the carotid arteries and it preferentially affects certain regions of circulation (e.g., the inner curve, close to side branches, and in the bulbs of the carotid artery [4–6]), suggesting that local mechanical factors might determine plaque development and growth. Plaque morphology and composition are evidently related to blood flow, which therefore influences the local predisposition to atherosclerosis progression, plaque rupture, and thrombosis. Furthermore, there is ample evidence that low wall shear stress is involved in plaque initiation and progression through various molecular mechanisms that influence endothelial cell morphology and function [7,8]. Atherosclerosis is considered to be a disease caused by a variety of clinical environmental factors and genetic factors. In recent years, numerous polymorphisms of genes related to atherosclerosis have been found by genome-wide association study (GWAS) and meta-analysis in large-scale studies [9–13]. On the other hands, other studies showed high wall shear stress is related to intraplaque hemorrhage and stroke [14,15]. Other hemodynamic parameters related to atherosclerosis include wall pressure, shear strain rates, and flow velocity.

Such hemodynamic characteristics were usually obtained by computational fluid dynamics (CFD). CFD is mechanical engineering field which is widely used in mechanical engineering to solve complex problems by analyzing fluid flow, heat transfer, and associated phenomena by using computer simulations. CFD is becoming a vital component in the design of industrial products and systems. Examples are aerodynamics and hydrodynamics of vehicles, power plants and turbines, electronic engineering, chemical engineering, external and internal environmental architectural design, marine and environmental engineering, hydrology, meteorology, and biomedical engineering. In recent years, CFD biomedical research is more accessible because high-performance hardware and software are easily available with advances in computer science.

Few studies have investigated the relationship between carotid plaque hemodynamic characteristics and risk of stroke in asymptomatic patients [14]. Therefore, in this study, we

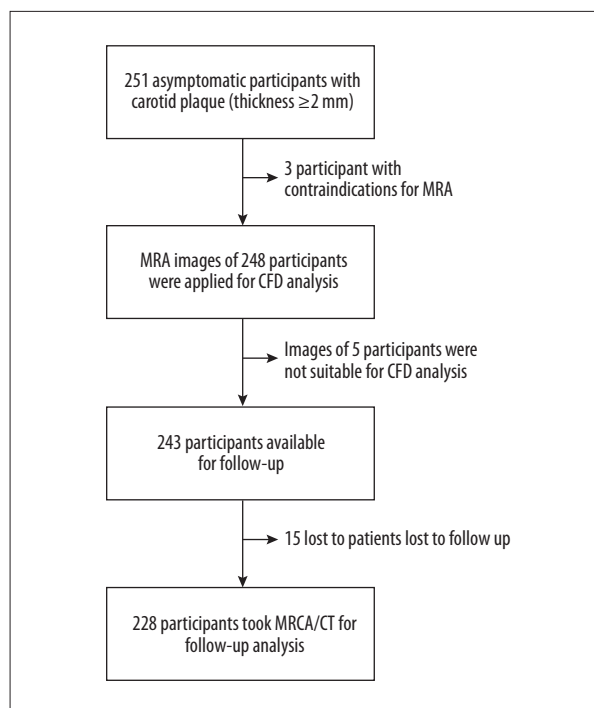


Figure 1. Flow chart of participants included and excluded for analysis.

aimed to investigate the relationship between hemodynamic parameters of asymptomatic carotid plaques by using CFD and magnetic resonance angiography (MRA), including flow velocity across the lesion, wall shear stress (WSS), wall pressure (WP), and the risk of stroke.

Material and Methods

Study population

This prospective study was performed at the Chinese PLA General Hospital, Beijing, China from March 2011 to June 2013. For the purpose of our study, asymptomatic participants with carotid plaque (thickness ≥ 2 mm) in one of the carotid arteries were enrolled. All participants were invited for an MRA of both carotid arteries. The exclusion criteria included: 1) images were not suitable for CFD analysis: the stenosis degree greater than 95% or less than 10%; and 2) contraindications for MRA: any electrically, magnetically, or mechanically activated implant, intracranial aneurysm clips (unless made of titanium), ferromagnetic surgical clips or staples, metallic foreign body in the eye, or pregnancy. Demographics, histories of common diseases (previously diagnosed or taking corresponding medications at baseline), and results of laboratory tests at baseline were collected from computerized medical records and ultrasound reports. Follow-up data were collected in June 2016. The primary endpoint was defined as a stroke based on

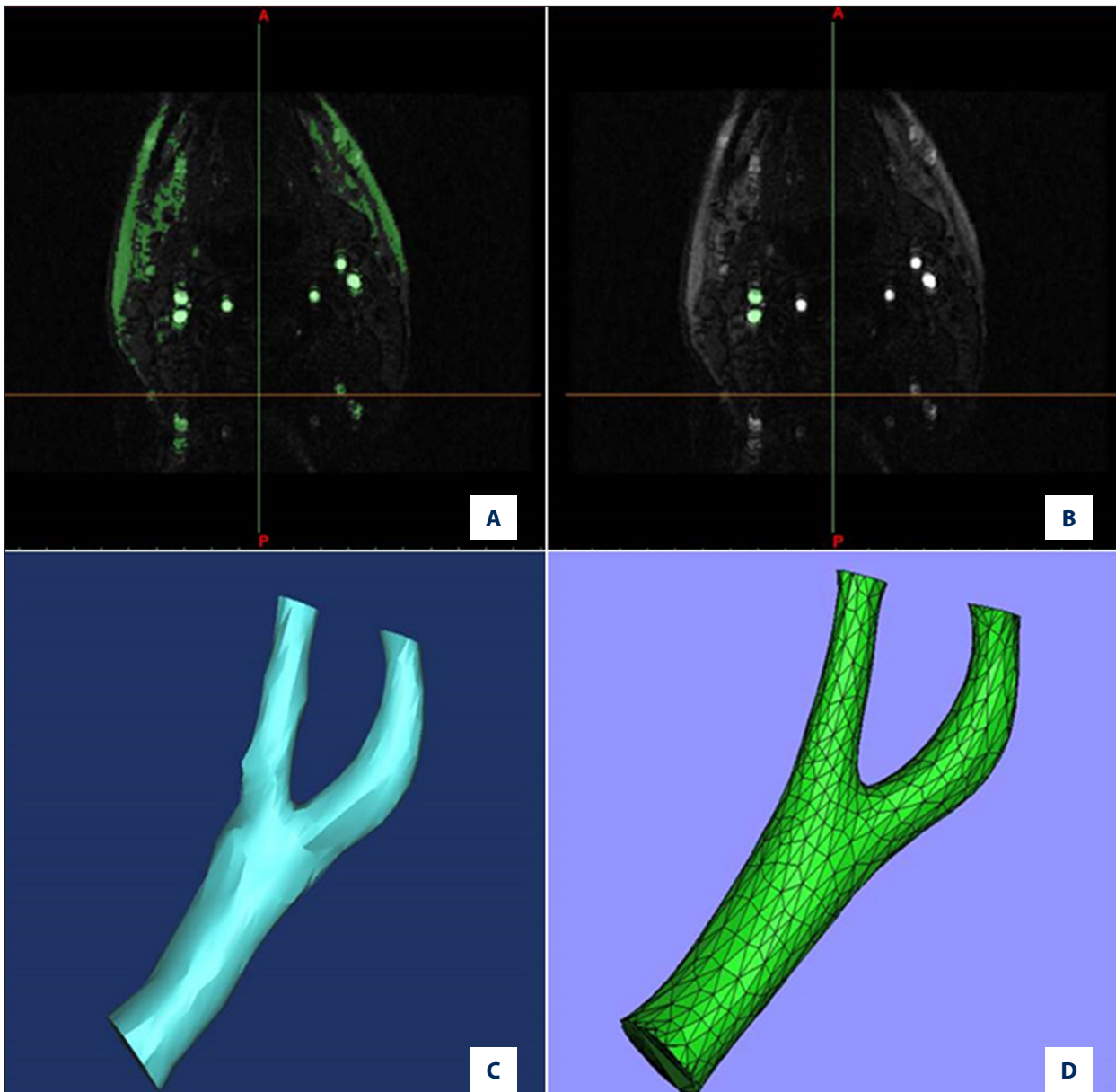


Figure 2. Reconstruction of 3D vascular model using MIMICS software based on MR data. (A) Thresholding of carotid artery images; (B) Mask of carotid artery images; (C) 3D vascular model constructed with MIMICS; (D) Remeshed model using 3-MATIC.

typical clinical symptoms and confirmed by follow-up brain CT or MRA. Secondary endpoints included any ischemic stroke or TIA, and all-cause death. A flow chart explaining the final data used for analysis is shown in Figure 1. The participants were divided into a stroke group and a non-stroke group according to follow-up data. Written informed consent had obtained from each participant included in the study. The study was approved by the Ethics Committee for Medical Research of the Chinese PLA General Hospital.

Magnetic resonance protocol and image analysis

Carotid plaques MRAs were obtained by a Signal 1.5T MR Systems (General-Electric Healthcare, Milwaukee, WI) using a bilateral phased-array surface coil with a slice thickness of 1.2 mm. MRA scan range was from the aortic arch to the skull base, and we selected the 4 cm within the scope of the original image of the carotid bifurcation (i.e., within the 4-cm scope of the CCA, ICA, and ECA). After the scan was completed, the Digital Imaging and Communications in Medicine (DICOM) format images were derived. All images were imported to the post-processing workstation ADW4.5-1 (General-Electric

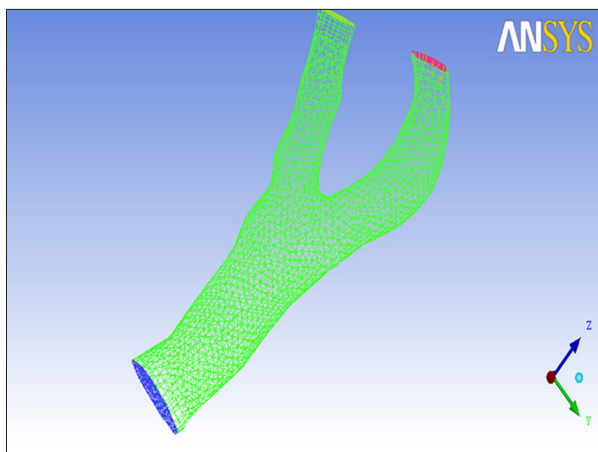


Figure 3. Global tetrahedral mesh elements of the carotid artery.

Healthcare, Milwaukee, WI) for image evaluation and analysis. Luminal area (LA) was defined as the area encompassed by the inner boundary of the intimal surface in plaque slices. Total vessel area (TVA) was defined by the outer boundary of the vessel. Wall area (WA) was calculated by the software, subtracting TVA from LA (WA=TVA-LA). A normalized wall index was then calculated (NWI=WA/TVA) [16].

Geometric modeling

Geometric modeling was performed by importing the DICOM format MRA data into reverse engineering 3D reconstruction software MIMICS (Materialise Inc., Belgium), by threshold segmentation (Figure 2A), region growing, and use of mask film editing (Figure 2B) tools to get a sense of vessels in the region of interest (ROI) mask by mimics the 3-dimensional (3D) transport calculation functions, connection of the extracted two-dimensional (2D) section, and generating a 3D carotid arteries geometric model (Figure 2C). we then imported the 3D models into the forward engineering software 3-MATIC to remesh the surface of the arteries (Figure 2D) and improve the quality of the grid.

CFD modeling

We imported STL format images into the ICEM-CFD software to identify the 3D space structure, and defined the 1-inlet, 2-outlets, the vessel wall, and other parts of arteries. Then, we set the parameters required for the tetrahedral mesh according to the size of the arteries. To guarantee the accuracy of the boundary of the target artery, we set up a 3-layer boundary calculate condition, and the growth factor was increased by 1.2 times. Global tetrahedral mesh elements of the carotid artery are shown in Figure 3.

We imported tetrahedral mesh files into a FLUENT model with ANSYS software and set the following boundary conditions:

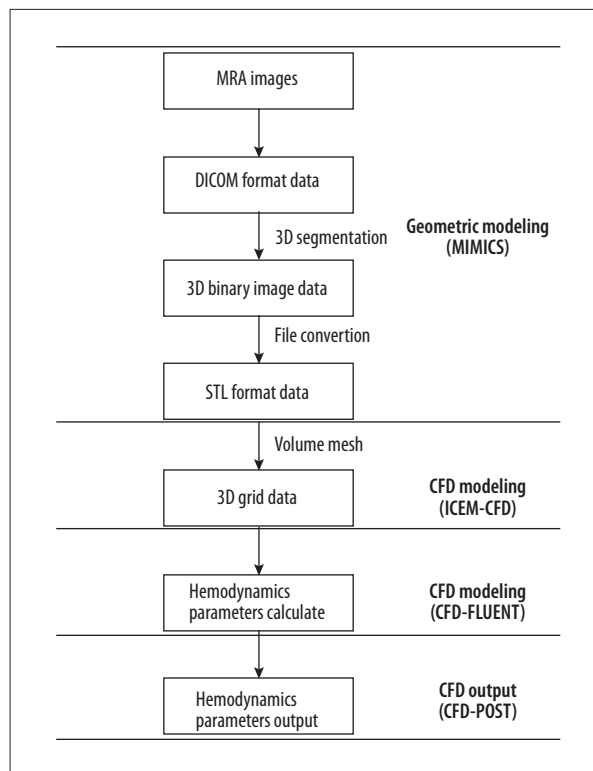


Figure 4. Work flow of CFD analysis.

(1) vascular wall characteristics: vascular walls were set to smooth, no penetration of rigid [17,18]; (2) blood characteristics: the blood flow was assumed laminar, incompressible, and Newtonian, with density of 1060 kg/m³ and viscosity of 0.0035Pas; (3) the inlet velocity was measured by MRA and the blood flow of internal and external carotid arteries were 55% and 45%, respectively [19]; and (4) the calculation was based on continuity equation and Navier-Storks equation [20].

The workflow of CFD analysis is shown in Figure 4

$$\frac{\partial u}{\partial x} + \frac{\partial v}{\partial y} + \frac{\partial w}{\partial z} = 0$$

$$\frac{\partial (\rho u)}{\partial t} + \text{div}(\rho u U) = \text{div}(\mu \text{grad} u) - \frac{\partial P}{\partial x} + S_u$$

$$\frac{\partial (\rho v)}{\partial t} + \text{div}(\rho v U) = \text{div}(\mu \text{grad} v) - \frac{\partial P}{\partial y} + S_v$$

$$\frac{\partial (\rho w)}{\partial t} + \text{div}(\rho w U) = \text{div}(\mu \text{grad} w) - \frac{\partial P}{\partial z} + S_w$$

Statistical analysis

All continuous variables are presented as means ±SD. The normal distribution test for continuous variables was conducted using the Kolmogorov-Smirnov test. Statistical analysis of

Table 1. Baseline characteristics of all participants.

	Stroke group (n=16)	Non-stroke group (n=212)	P
Age	57.88±7.79	59.55±8.73	0.625
Male	10 (62.50)	110 (51.89)	0.442
Smoke	6 (37.5)	88 (41.51)	0.575
Medical history			
Coronary heart disease	6 (37.50)	74 (34.91)	0.401
Hypertension	8 (50.00)	136 (64.15)	0.422
Diabetes	6 (37.50)	116 (54.72)	0.068
Arrhythmia	2 (12.50)	54 (25.47)	0.393
Hyperlipidemia	4 (25.00)	60 (28.30)	0.607
Physical examination			
HR	77.00±12.86	75.55±10.38	0.739
SBP	124.38±17.68	125.90±25.63	0.875
DBP	72.25±8.28	76.84±15.25	0.420
BMI	26.31±6.95	24.43±4.29	0.340
Laboratory tests			
ALT	25.26±12.84	39.36±15.32	0.600
AST	35.05±16.11	42.70±17.16	0.342
γ-GT	43.14±23.62	61.16±29.27	0.417
Cr	78.65±25.67	110.74±45.95	0.220
BUN	7.26±3.69	7.05±2.50	0.855
TG	1.48±0.29	1.31±0.75	0.562
T-CH	3.68±0.76	4.03±1.43	0.504
HDL	0.92±0.27	0.98±0.29	0.540
LDL	1.99±0.58	2.34±0.98	0.332
Hb	129.00±14.96	113.19±29.37	0.152
RBC	4.21±0.47	3.89±0.99	0.386
WBC	7.51±1.24	8.49±2.00	0.496
PLT	209.50±54.87	201.61±83.39	0.852

Values are means ±SD for continuous variables and percentages for dichotomous variables.

normal distribution data was performed using an unpaired *t* test between 2 groups. Non-normal distribution data were analyzed using the Mann-Whitney U test for continuous variables and the χ^2 test for discrete variables. The influence of morphology and hemodynamics characteristics was evaluated using univariate logistics regression models. Results from logistics models are expressed as hazard ratios with 95%

confidence intervals. Receiver operator characteristic curve (ROC) and C-statistic testing were utilized to assess the performance of the constructed model in comparison with a previous published model. All tests were carried out using SPSS version 17.0 (SPSS Inc., Chicago, IL, USA) statistical software. Differences were considered statistically significant at a two-tailed P value of less than 0.05.

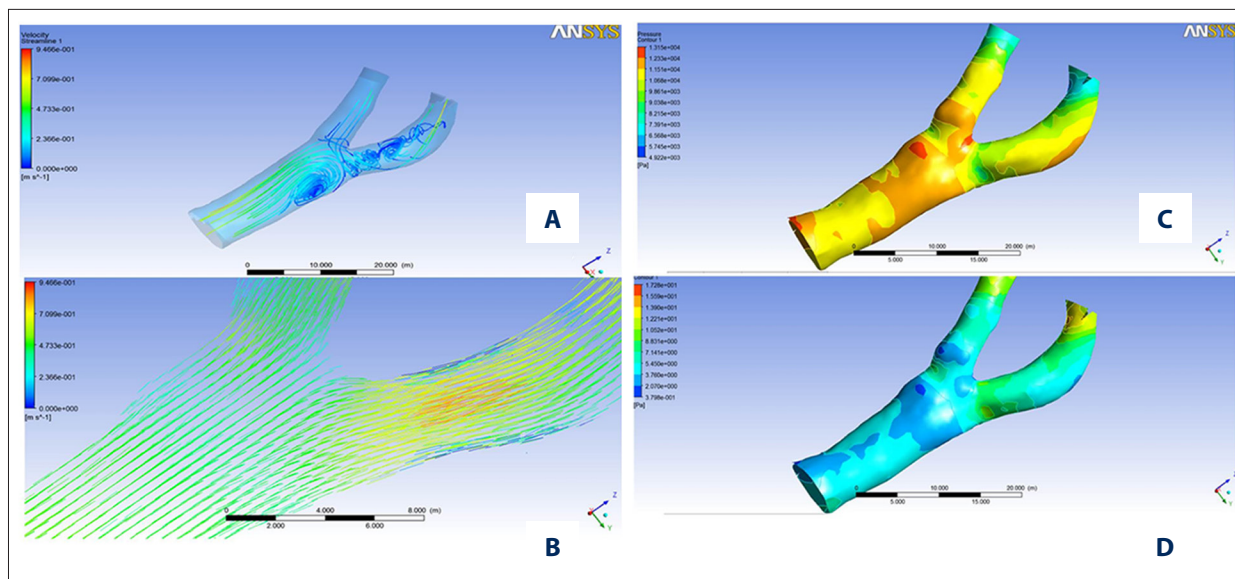


Figure 5. An example of CFD analysis in carotid artery. (A) Streamline pictures of the flow; (B) Velocity vector picture; (C) Contours of WP; (D) Contours of WSS.

Table 2. Qualitative of MRA and Hemodynamic parameters of all participants.

	Stroke group (n=16)	Non-stroke group (n=212)	P
LA (mm ²)	32.32±9.58	34.20±11.11	0.124
WA (mm ²)	38.49±11.63	37.23±13.32	0.139
TVA (mm ²)	70.82±10.81	71.43±14.95	0.749
NWI	0.64±0.15	0.47±0.19	0.043
WSS (Pa)	7.87±1.34	5.86±2.14	0.013
WP (Pa)	-1015.75±109.99	-961.68±199.07	0.467

Results

Baseline

We included 228 participants with asymptomatic carotid plaque in this prospective study. The study population included 120 men (52.63%) and 108 women (47.37%), the mean age was 59.21±8.48 years, and the mean follow-up duration was 1147.56±224.84 days. The follow-up results showed 16 of 228 patients with asymptomatic carotid plaques had experienced a stroke. The participants were divided into a stroke group and a non-stroke group according to whether stroke had occurred. Detail information on demographics, medical history, physical examination, and results of laboratory tests of the 2 groups are shown in Table 1. There were no significant differences between the 2 groups in terms of age, sex, history of smoking, medical history, physical examination, or laboratory test results.

Hemodynamic and MRA characteristics of carotid artery

Figure 5A is a streamlined picture of the flow, showing turbulent regions with obvious velocity slowing above and below the plaques. Local amplification of the velocity vector (Figure 5B) shows the blood flow velocity was accelerated in the stenosis region. Contours of WP (Figure 5C) show the wall pressure was gradually decreased from the inlet to the outlets of the carotid artery. However, the WP of the bifurcation site of the common carotid artery was abnormally high, and atherosclerotic lesions showed decreased WP. On the other hand, contours of WSS (Figure 5D) showed the uneven distribution of WSS of the carotid artery. High WSS appeared in the center area of the plaque sites. Table 2 shows the qualitative assessment of MRA and hemodynamic parameters of all participants. The stroke group and non-stroke group were similar with respect to LA, WA, and TVA. The NWI of the stroke group was higher than in the non-stroke group (0.54±0.15

Table 3. Logistics regression analysis of hemodynamic and MRA characteristics of carotid artery.

	OR	95% Confidence interval	P
LA (mm ²)	0.863	0.836–0.917	0.353
WA (mm ²)	1.082	1.063–1.105	0.298
TVA (mm ²)	0.980	0.924–1.022	0.322
NWI	3.472	2.943–4.096	0.011
WSS (Pa)	6.974	1.070–45.453	0.042
WP (Pa)	1.005	0.997–1.013	0.239

Table 4. Area under the receiver operating characteristic curve for WSS, NWI and WSS+NWI.

Factors	Area	SE	95%CI	Youden's index	Sensitivity	Specificity
WSS	0.772	0.079	0.618–0.926	0.649	87.50	77.42
NWI	0.798	0.071	0.660–0.937	0.520	87.50	64.52
WSS+NWI	0.903	0.051	0.804–1.000	0.774	100.00	77.42

vs. 0.52 ± 0.19 , $p=0.043$). Qualitative assessment of hemodynamic parameters showed no significant difference between the stroke group and non-stroke group in WP; however, WSS of the stroke group was higher than in the non-stroke group (7.87 ± 1.34 vs. 5.86 ± 2.14 , $P=0.013$).

Logistics regression analysis

Logistics regression analysis indicated that NWI and WSS were associated with the development of carotid plaques (Table 3). Carotid artery with higher NWI had 3.472 times more chance of being associated with stroke. High WSS increased the chance of the stroke by 6.974 times. Other hemodynamic and MRA characteristics of carotid artery did not show significant associations with the risk of stroke.

ROC analysis

To assess the predictive utility of WSS, NWI, and WSS+NWI, we compared the ROC curves of these 3 parameters. The area under the ROC curve values for WSS, NWI, and WSS+NWI were 0.772, 0.798, and 0.903, respectively (Table 4). WSS+NWI predicted the onset of stroke better than WSS and NWI ($P<0.05$), with no statistically significant differences between WSS and NWI (Figure 6). P values close to 1 were associated with higher risk of stroke.

Discussion

The present study used morphologic data derived from MRA and geometric parameter data obtained by CFD to examine the

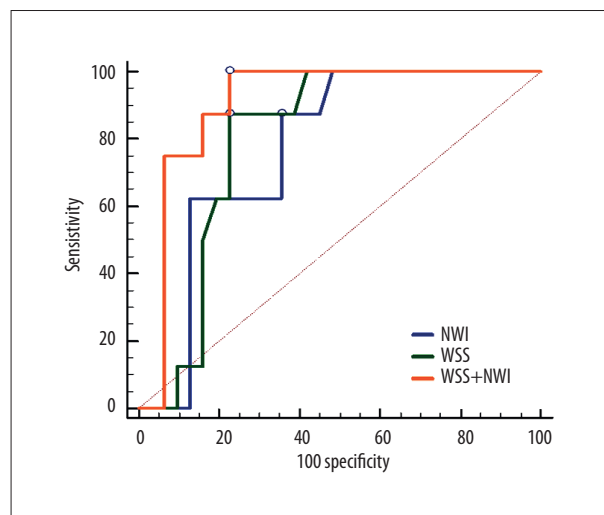


Figure 6. Receiver operating characteristic curve for NWI, WSS, and WSS+NWI (the areas under the curve were 0.798, 0.772, and 0.903, respectively).

relationship between carotid plaques and the risk of stroke in patients with asymptomatic carotid plaques. Our study shows that carotid atherosclerosis is a dynamic and progressive disease. Of the 228 participants with asymptomatic carotid plaques, 16 (7.02%) had stroke in the territory of the carotid artery, which was comparable to Kakkos's and Chung's studies [21,22]. Additionally, the probability of stroke was much lower than in Sadat's study [23]. The difference may be that Sadat's cohort had suffered a stroke before and were not asymptomatic as such.

For the CFD analysis, most of the previous studies used standard flow velocity [19]. Instead of this, we used person-specific inlet flow velocity measured by MRA, which allowed us to get more accurate parameters of fluid dynamics.

Several studies have investigated the association between carotid plaques progression and risk of cerebrovascular events in patients with asymptomatic carotid stenosis [1,22,24–28]. These risk factors including age, sex [29], severity of stenosis [22,25,26], increased plaque area [22], carotid artery end-diastolic velocity [21], systolic blood pressure [25], and increased serum creatinine [22,25]. Furthermore, genetics and epigenetics factors in atherosclerosis cannot be ignored [30,31]. Our analysis suggests that plaque morphology characteristics NWI and hemodynamics parameter WSS are independent risk factors for the progression from asymptomatic to stroke. Logistics regression analysis and ROC curve suggest that the combination of NWI and WSS is better at predicting the risk of stroke.

During the early stages of atherosclerotic plaque growth, the vessel may remodel and accommodate plaque growth without compromising luminal size. There are few plaque morphology characteristics, such as WA, used to assess plaques. Clinical trials have shown that in human carotid arteries, luminal stenosis has limited value as an indicator of atherosclerotic plaque vulnerability, enabling prediction of only 1 of 10 strokes in asymptomatic patients [32]. Plaque burden, which is represented by plaque volume and maximum wall area (MWA), as a direct measure of the lesion itself, may have substantial usefulness in the assessment of atherosclerosis [33]. Studies have shown NWI is a sensitive factor for early detection of carotid atherosclerosis plaques, and it can reflect the progression of plaque more accurately than other morphology characteristics such as LA and WA. Calculated as WA/TVA , NWI contains information about lumen stenosis and thickening of the wall, which make NWI is the most effective indicator for evaluating the severity of atherosclerosis. NWI increases the comparability between different individuals and different vessel areas. Furthermore, it can avoid the difference in the wall area caused by different vascular thicknesses [34]. Therefore, NWI may also be used as a dynamic index to measure the dynamic changes of plaques.

Prediction of plaque rupture before the event is a major clinical challenge. Even though morphology characteristics of plaques were thought to relate to the progression of local lesion, as mentioned above, plaque rupture is not solely dependent on plaque morphology, and other local factors are probably involved. As a consequence of improvements in imaging of atherosclerosis and in computational power, there has been increasing interest in the role of biomechanical forces in plaque rupture [35]. There is increasing evidence that hemodynamic factors are important in the atherogenic process and in the development of unstable plaque and thromboembolic stroke.

Disturbances of hemodynamics are thought to have a role in several aspects of this process, particularly in the causation of plaque rupture and in the formation of surface thrombus.

The follow-up radiographic results confirmed that the culprit sites were consistent with the regions of high WSS. WSS is the parallel frictional force exerted by blood flow on the endoluminal surface of the arterial wall. The magnitude of WSS is influenced by changes in luminal geometry, blood flow velocity, and plasma viscosity [36]. There are 2 different views on the role of WSS in atherosclerosis. Although studies suggested that a certain degree of high WSS has anti-atherosclerosis effect [37], the increase of WSS is not necessarily a protective factor for atherosclerosis [38]. Lovett [39] showed that plaque ruptures more frequently in the upper side of the lumen, which is affected by the high WSS and leads to the production of vulnerable plaque with a thin fibrous cap. Studies of clinical pathological autopsies also showed that plaque rupture mainly occurred in the upper side of the lesion, consistent with the area of high WSS. Although the absolute value of the WSS is not enough to directly damage the structure of the fiber cap, the increased WSS in the upper side of the lesion is the primary factor causing rupture of the plaque [40].

Studies have confirmed that WSS is associated with regulation of many vascular functions, such as maintenance of acute vessel tone, vascular permeability, adhesion of leukocytes, development of blood vessels, and secretion of pro-thrombotic and antithrombotic signaling molecules [41,42]. Activated ECs produce chemokines, cytokines, and adhesion molecules that interact with leukocytes and platelets, and target inflammation to specific tissues as a host defense mechanism [43]. Balaguru's team developed a versatile model based on CFD simulation to explore the shear stress-associated changes of biological function in endothelial cells (ECs) [44]. Cell morphology, cytoskeletal arrangement, cell death, reactive oxygen species profile, nitric oxide production, and disturbed flow markers under certain WSS condition were assessed. They observed a 2–4-fold increase in VEGFR2 expression in high-WSS regions, but the increase in expression was not observed in low-WSS areas. MCP-1 involved in the recruitment of leukocytes plays a significant role in the development of atherosclerotic plaque formation. There was a 4-fold increase in expression observed in high-WSS regions. HIF1 alpha expression is used as a marker for hypoxia. There was a 2-fold increase in expression of HIF1- α in high-WSS regions, and a less than 2-fold increase in low-WSS areas.

Locally high WSS might promote transformation of stable subtypes to vulnerable plaques. Previous studies showed higher maximum shear stress is associated with intraplaque hemorrhage and calcifications [45]. Plaques that contain a large lipid-rich necrotic core, intraplaque hemorrhage, inflammation,

and/or are covered by a thin fibrous cap are considered the most vulnerable to rupture. In animal studies and small case studies, an association between WSS and plaque composition was observed. Although low WSS may induce plaque initiation, it has been hypothesized that plaque destabilization can be caused by high shear stress on the plaque. Tuentner's study evaluated the association between shear stress and plaque components in asymptomatic persons.

Conclusions

We found that the combination of plaque morphology characteristics NWI and hemodynamics parameter WSS can improve the ability to identify patients at highest risk of rapid

disease progression and may predict the risk of stroke in patients with asymptomatic carotid plaques. More prospective studies with larger sample sizes are necessary to validate the findings of this study and to discover new risk factors for imaging and fluid mechanics.

Conflict of interest

We do not have anything to disclose regarding conflict of interest with respect to this manuscript.

Acknowledgments

We are grateful to staff in the Department of Cardiology, Chinese PLA General Hospital.

References:

1. de Weerd M, Greving JP, Hedblad B et al: Prevalence of asymptomatic carotid artery stenosis in the general population: An individual participant data meta-analysis. *Stroke*, 2010; 41: 1294–97
2. Sabetai MM, Tegos TJ, Nicolaides AN et al: Hemispheric symptoms and carotid plaque echomorphology. *J Vasc Surg*, 2000; 31: 39–49
3. Makaryus AN, Phillips LM, Wright P et al: Mandatory diagnostic angiography for carotid artery stenosis prior to carotid artery intervention. *J Interv Cardiol*, 2009; 22: 16–21
4. Dempsey RJ, Diana AL, Moore RW: Thickness of carotid artery atherosclerotic plaque and ischemic risk. *Neurosurgery*, 1990; 27: 343–48
5. Asakura T, Karino T: Flow patterns and spatial distribution of atherosclerotic lesions in human coronary arteries. *Circ Res*, 1990; 66: 1045–66
6. Rothwell PM: Carotid artery disease and the risk of ischaemic stroke and coronary vascular events. *Cerebrovasc Dis*, 2000; 10(Suppl. 5): 21–33
7. Sadat U, Teng Z, Gillard JH: Biomechanical structural stresses of atherosclerotic plaques. *Expert Rev Cardiovasc Ther*, 2010; 8: 1469–81
8. Cecchi E, Giglioli C, Valente S et al: Role of hemodynamic shear stress in cardiovascular disease. *Atherosclerosis*, 2011; 214: 249–56
9. Starcevic JN, Petrovic D: Carotid intima media-thickness and genes involved in lipid metabolism in diabetic patients using statins – a pathway toward personalized medicine. *Cardiovasc Hematol Agents Med Chem*, 2013; 11(1): 3–8
10. Turner AW, Martinuk A, Silva A et al: Functional analysis of a novel genome-wide association study signal in smad3 that confers protection from coronary artery disease. *Arterioscler Thromb Vasc Biol*, 2016; 36(5): 972–83
11. Kariz S, Milutinovic A, Bregar D et al: The interleukin-1 receptor antagonist gene and the inhibitor of kappa b-like protein gene polymorphisms are not associated with myocardial infarction in slovene population with type 2 diabetes. *Coll Antropol*, 2007; 31: 503–7
12. Reynolds LM, Wan M, Ding J et al: DNA methylation of the aryl hydrocarbon receptor repressor associations with cigarette smoking and subclinical atherosclerosis. *Circ Cardiovasc Genet*, 2015; 8: 707–16
13. Declerck K, Szarc vel Szi K, Palagani A et al: Epigenetic control of cardiovascular health by nutritional polyphenols involves multiple chromatin-modifying writer-reader-eraser proteins. *Curr Top Med Chem*, 2016; 16: 788–806
14. Tuentner A, Selwaness M, Arias Lorza A et al: High shear stress relates to intraplaque haemorrhage in asymptomatic carotid plaques. *Atherosclerosis*, 2016; 251: 348–54
15. Leng X, Scalzo F, Ip HL et al: Computational fluid dynamics modeling of symptomatic intracranial atherosclerosis may predict risk of stroke recurrence. *PLoS One*, 2014; 9: e97531
16. Bianda N, Di Valentino M, Periat D et al: Progression of human carotid and femoral atherosclerosis: A prospective follow-up study by magnetic resonance vessel wall imaging. *Eur Heart J*, 2012; 33: 230–37
17. Schirmer CM, Malek AM: Prediction of complex flow patterns in intracranial atherosclerotic disease using computational fluid dynamics. *Neurosurgery*, 2007; 61: 842–51; discussion 852
18. Mohammadi H, Bahramian F: Boundary conditions in simulation of stenosed coronary arteries. *Cardiovasc Eng*, 2009; 9: 83–91
19. Long Q, Xu XY, Kohler U et al: Quantitative comparison of CFD predicted and MRI measured velocity fields in a carotid bifurcation phantom. *Biorheology*, 2002; 39: 467–74
20. Shen F, Li X, Li PC: Study of flow behaviors on single-cell manipulation and shear stress reduction in microfluidic chips using computational fluid dynamics simulations. *Biomicrofluidics*, 2014; 8: 014109
21. Chung H, Jung YH, Kim KH et al: Carotid artery end-diastolic velocity and future cerebro-cardiovascular events in asymptomatic high risk patients. *Korean Circ J*, 2016; 46: 72–78
22. Kakkos SK, Nicolaides AN, Charalambous I et al, Asymptomatic Carotid Stenosis and Risk of Stroke (ACSRS) Study Group: Predictors and clinical significance of progression or regression of asymptomatic carotid stenosis. *J Vasc Surg*, 2014; 59: 956–967e1
23. Sadat U, Teng Z, Young VE et al: Association between biomechanical structural stresses of atherosclerotic carotid plaques and subsequent ischaemic cerebrovascular events – a longitudinal *in vivo* magnetic resonance imaging-based finite element study. *Eur J Vasc Endovasc Surg*, 2010; 40: 485–91
24. Ballotta E, Da Giau G, Santarelli G et al: Natural history of symptomatic and asymptomatic carotid artery occlusion contralateral to carotid endarterectomy: A prospective study. *Vasc Endovasc Surg*, 2007; 41: 206–11
25. Nicolaides AN, Kakkos SK, Kyriacou E et al, Asymptomatic Carotid Stenosis and Risk of Stroke (ACSRS) Study Group: Asymptomatic internal carotid artery stenosis and cerebrovascular risk stratification. *J Vasc Surg*, 2010; 52: 1486–96e1–5
26. Singh TD, Kramer CL, Mandrekar J et al: Asymptomatic carotid stenosis: Risk of progression and development of symptoms. *Cerebrovasc Dis*, 2015; 40: 236–43
27. Hirt LS: Progression rate and ipsilateral neurological events in asymptomatic carotid stenosis. *Stroke*, 2014; 45: 702–6
28. Hollander M, Bots ML, Del Sol AI et al: Carotid plaques increase the risk of stroke and subtypes of cerebral infarction in asymptomatic elderly: The Rotterdam study. *Circulation*, 2002; 105: 2872–77
29. Wendorff C, Wendorff H, Kuehn A et al: Impact of sex and age on carotid plaque instability in asymptomatic patients—results from the munich vascular biobank. *Vasa*, 2016; 45(5): 411–16
30. Tibaut M, Petrovic D: Oxidative stress genes, antioxidants and coronary artery disease in type 2 diabetes mellitus. *Cardiovasc Hematol Agents Med Chem*, 2016; 14(1): 23–38
31. Petrovic D: The role of vascular endothelial growth factor gene as the genetic marker of atherothrombotic disorders and in the gene therapy of coronary artery disease. *Cardiovasc Hematol Agents Med Chem*, 2010; 8: 47–54

32. Endarterectomy for asymptomatic carotid artery stenosis. Executive committee for the asymptomatic carotid atherosclerosis study. *JAMA*, 1995; 273: 1421–28
33. Zhang S, Cai J, Luo Y et al: Measurement of carotid wall volume and maximum area with contrast-enhanced 3d mr imaging: Initial observations. *Radiology*, 2003; 228: 200–5
34. Zhao X, Miller ZE, Yuan C: Atherosclerotic plaque imaging by carotid MRI. *Curr Cardiol Rep*, 2009; 11: 70–77
35. Brown AJ, Teng Z, Evans PC et al: Role of biomechanical forces in the natural history of coronary atherosclerosis. *Nat Rev Cardiol*, 2016; 13: 210–20
36. Chiu JJ, Chien S: Effects of disturbed flow on vascular endothelium: Pathophysiological basis and clinical perspectives. *Physiol Rev*, 2011; 91: 327–87
37. Dai G, Vaughn S, Zhang Y et al: Biomechanical forces in atherosclerosis-resistant vascular regions regulate endothelial redox balance via phosphoinositol 3-kinase/akt-dependent activation of nrf2. *Circ Res*, 2007; 101: 723–33
38. Groen HC, Gijssen FJ, van der Lugt A et al: Plaque rupture in the carotid artery is localized at the high shear stress region: A case report. *Stroke*, 2007; 38: 2379–81
39. Lovett JK, Rothwell PM: Site of carotid plaque ulceration in relation to direction of blood flow: An angiographic and pathological study. *Cerebrovasc Dis*, 2003; 16: 369–75
40. Sui B, Gao P, Lin Y et al: Hemodynamic parameters distribution of upstream, stenosis center, and downstream sides of plaques in carotid artery with different stenosis: A MRI and CFD study. *Acta Radiol*, 2015; 56: 347–54
41. Traub O, Berk BC: Laminar shear stress: Mechanisms by which endothelial cells transduce an atheroprotective force. *Arterioscler Thromb Vasc Biol*, 1998; 18: 677–85
42. Ene-Iordache B, Remuzzi A: Disturbed flow in radial-cephalic arteriovenous fistulae for haemodialysis: Low and oscillating shear stress locates the sites of stenosis. *Nephrol Dial Transplant*, 2012; 27: 358–68
43. Deanfield JE, Halcox JP, Rabelink TJ: Endothelial function and dysfunction: Testing and clinical relevance. *Circulation*, 2007; 115: 1285–95
44. Balaguru UM, Sundaresan L, Manivannan J et al: Disturbed flow mediated modulation of shear forces on endothelial plane: A proposed model for studying endothelium around atherosclerotic plaques. *Sci Rep*, 2016; 6: 27304
45. Tuenter A, Selwaness M, Arias Lorza A et al: High shear stress relates to intraplaque haemorrhage in asymptomatic carotid plaques. *Atherosclerosis*, 2016; 251: 348–54